

A versatile strategy for hybridizing small experimental and large simulation data: A case for ceramic tape-casting process

Jeong-Hun Kim^{a,1}, Hyunseok Ko^{b,1}, Dong-Hun Yeo^c, Zeehoon Park^c, Upendra Kumar^b, Kwan-Hee Yoo^a, Aziz Nasridinov^{a,*}, Sung Beom Cho^{d,e,*}

^a Department of Computer Science, Chungbuk National University, Cheongju 28644, Republic of Korea

^b Center of Materials Digitalization, Korea Institute of Ceramic Engineering and Technology, Jinju 52851, Republic of Korea

^c Ceramic Test-bed Center, Korea Institute of Ceramic Engineering and Technology, Icheon 17303, Republic of Korea

^d Department of Materials Science and Engineering, Ajou University, Suwon 16499, Republic of Korea

^e Department of Energy Systems Research, Ajou University, Suwon 16499, Republic of Korea



ARTICLE INFO

Keywords:

Machine learning
Simulation
Data deficiency
Inverse design
Tape-casting

ABSTRACT

In manufacturing industry, finding optimal design parameters for targeted properties has traditionally been guided by trial and error. However, limited data availability to few hundreds sets of experimental data in typical materials processes, the machine-learning capabilities and other data-driven modeling (DDM) techniques are too far from it to be practical. In this study, we show how a versatile design strategy, tightly coupled with physics-based modeling (PBM) data, can be applied to small set of experimental data to improve the optimization of process parameters. Our strategy uses PBM to achieve augmented data that includes essential physics: in other words, the PBM data allows the inverse design model to ‘learn’ physics, indirectly. We demonstrated the accuracy of both forward-prediction and inverse-optimization have been dramatically improved with the help of PBM data, which are relatively cheap and abundant. Furthermore, we found that the inverse model with augmented data can accurately optimize process parameters, even for ones those were not considered in the simulation. Such versatile strategy can be helpful for processes/experiments for the cases where the number of collectable data is limited, which is most of the case in industries.

1. Introduction

Inverse design is becoming more significant in materials-related industry for designing complex products and processes [1]. The inverse design technique provides a solution of design parameters for the desired performance, which aids in expediting the development process and solving scientific challenges [2]. For a long time, inverse design has been tried by the combination of optimization technique and physics-based modeling (PBM) [3,4]. This PBM is numerically constructed based on the scientific knowledges on materials and processes. However, the compete inverse design often meets a challenge due to the numerical stability, huge computation cost, and accuracy of the numerical model, depending on the accumulated scientific knowledge in the field [5]. Thereby a meaningful inverse design is available in only handful fields. Recently, machine learning is rising as the alternative solution for the inverse design [6]. The machine learning predicts outcomes using a

statistical method on a collected experimental data, known as a data-driven modeling (DDM) [7–10]. The DDM is beneficial for highly nonlinear system with complex variables and it proved their success in diverse fields such as production management and other commercial applications [10]. However, even the state-of-the-art DDM has often met with limited success in materials-related domain due to their large experimental data requirements, poor physical interpretability and consistency, and their lack of generalizability to out of data-sampling-boundary [9]. Most recently, some studies introduced physically meaningful constraints (i.e., features) in DDM models, to compensate the drawback of lacking physics in DDM [11–13].

Interestingly, these two representative modeling approaches have complimentary nature in perspective of data collection. To exploit the predictive power of DDM, the biggest hurdle is collecting a large amount of experimental data, which is very expensive in materials-related field. Most of the dataset for the materials-related field do not exceed more

* Corresponding authors.

E-mail addresses: aziz@chungbuk.ac.kr (A. Nasridinov), csb@ajou.ac.kr (S.B. Cho).

¹ These authors contributed equally.

than hundreds, and this is usually not enough to obtain enough accuracy for the prediction. Various strategies such as SMOTE [14] and GAN [15] have been proposed to solve this problem. However, the limitations are clear that these data can easily result in a model with overfitting and over-sensitivity to outliers, especially when the size of preset data is too small and the features are highly correlated. On the other hand, the PBM can generate tremendous simulation dataset based on the scientific knowledge. This large simulation dataset based on PBM has been used for training another machine learning model, as known as surrogate model, to obtain simulation result instantly or analyze the variable correlation [16–19]. However, this PBM-based dataset is usually not as accurate as experimental data and often not commensurate with experimental data [20]. For instance, the simulation of tape-casting process for reliable inverse design is still challenging even though it is one of the oldest and popular forming techniques for ceramic materials. Many of experimental variables should be oversimplified and complex fluid dynamic behavior cannot be described well. Nonetheless, this simulation dataset has been only predictive way to try the inverse design for a long time.

In this study, we propose a versatile strategy for inverse design to overcome the imbalanced data and accuracy problem of DDM and PBM by hybridizing feature attenuated from small experiment preset data and surrogate model from physics-based simulation. It is demonstrated that the accuracy of both forward-prediction and inverse-optimization of DDM have been dramatically improved with the assistance of surrogate model from PBM. Interestingly, even though the PBM capture partial physical principles, the accuracy for inverse design of non-shared parameters (i.e., not included in simulation model) is improved which implies the proposed model can be powerful searching for the optimal process parameters.

2. Preliminaries

2.1. Experimental dataset

To address the inverse design problem mentioned in Section 1, a tape casting process has been selected for a representative case. Tape casting

is one of the classic ceramic manufacturing processes, and its process is depicted in Fig. 1. In this process, the ceramic slurry is first prepared in a reservoir by mixing ceramic powder, binder, and defoamer. Hereafter, the powder contents are represented as the powder-to-binder ratio (P/B ratio) for the simplicity. The resulting slurry becomes a well-dispersed homogenized mixture of solvent and powder. Then the slurry is fed through the gap between rollers, also known as doctor blade. The fed slurry is staged on a supporting film and conveyed to drying zone (in an order of meters per minute) with multiple heating elements of temperature ranged from 50 to 100 °C. Lastly, the dried tape is then measured for its thickness by an automated sensor. The experimental tape casting datasets are retrieved from the test-bed (Icheon, S. Korea), and further details of manufacturing processes are described elsewhere [21]. The total 89 of experimental dataset was collected from the manufacturing processes, and its raw data are presented in Supporting Information, SI. 1.

High-quality experimental materials data would be ideal for training the data-driven models; unfortunately, experimental data are typically costly to obtain (requires time-consuming changes in apparatus settings and cleaning) and limited parametric variations are viable in practice. Thus 89 experimental data are rather considered small and inhomogeneous. In other words, this experimental dataset is biased, distracting data-driven modeling for the tape casting process. Consequently, data-driven models trained on this dataset are overfitted, which degrades is optimized for some parameters that have a high correlation with the process result; thus, the inverse design converges to many local optimums by the remaining parameters, leading to a multi-solution problem with high complexity.

2.2. Simulation settings

To estimate the predictability of conventional physics-based simulation, finite element method (FEM) simulations were carried out using COMSOL Multiphysics package to model the doctor blade part of the tape casting process, with the exclusion of drying and the rest of the procedure. Note that only part of the parameters (viscosity, coating speed, and bladegap) is considered in the FEM-based model, namely

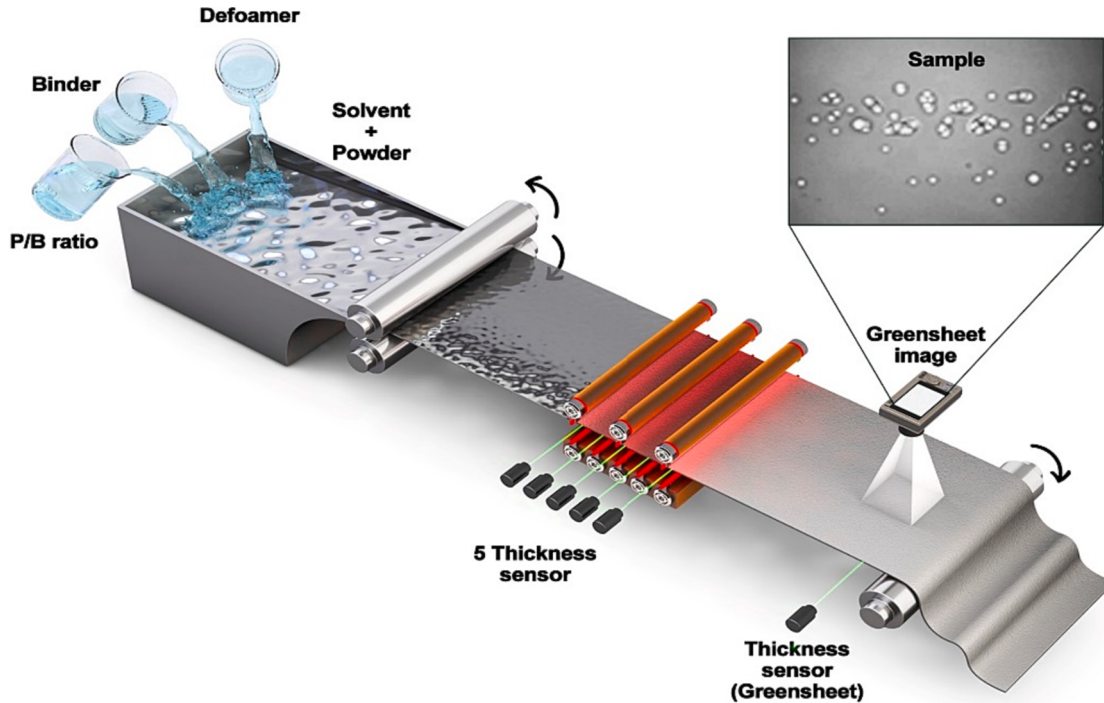


Fig. 1. The schematic of tape casting process.

shared-parameters. The rest of parameters, such as P/B ratio and binder, are noted as non-shared parameters, which is not implemented the FEM model directly. The schematic illustration of the model is depicted in Fig. 2(a), where slurry was introduced on one-end with a rate of coating speed. The Two-Phase Flow, Level Set coupling module is employed to evaluate the laminar flow of fluid (slurry) and air under gravitational environment. Further details of FEM model are presented in Supporting Information, SI. 2.

To examine the validity of the FEM simulation results, the FEM simulation results are compared to the experimental data, as shown in Fig. 2(b). The correspondence of experimental data to equivalent simulation data are presented for 89 pairs. As depicted by the fitted polynomial, the simulation data does not show a 1-to-1 correlation to experimental data, but a distinctive correlation is observed. The huge discrepancy is not a surprise, as we only modeled the initial part of the tape casting process, and not considered physics from rest of the processes (e.g., heat dissipation of the heat, volumetric swelling and induced strain during the solidification), and the effectiveness of non-shared parameters. This observation indicates that the partial physics of tape casting modeled with shared parameters has a clear correlation with the experimental data, which makes the proposed FEM simulation valid for the tape casting. In addition, the observation implies that the remaining physics of tape casting causes discrepancies between experimental data and simulations.

3. Proposed strategy

Motivated by the observation in Section 2.2, we here propose a versatile strategy to provide inverse design by hybridizing physics-based and data-driven models. Fig. 3(a) illustrates an overview of the proposed

strategy which consists of three parts: 1) forward prediction model construction; 2) data augmentation using the forward prediction model; and 3) inverse design (i.e., process modeling) based on the augmented dataset. As shown in Fig. 3(a), we partition 89 experimental data into 70 % training and 30 % validation sets. Subsequently, we construct the forward prediction model in which PBM based on FEM simulation and DDM based on the experimental data are hybridized. In the data augmentation part, we design homogeneous experimental data by considering shared (viscosity, coating speed, and bladegap) and non-shared (P/B ratio and binder) parameters. Then, we generate the designed experimental data using the forward prediction model. Lastly, we provide an inverse design by modeling the process based on the augmented experimental data.

3.1. Forward prediction model

To incorporate the advantages of PBM and DDM, we propose a deep learning-based forward prediction (FP) model. As shown in Fig. 4, the proposed FP model consists of two networks, physics imitation network (PIN) and data-driven modeling network (DDMN). More precisely, PIN learns process patterns of shared parameters based on FEM simulation. These process patterns represent various physics for the shared parameters designed by FEM simulation. On the other hand, DDMN learns data-driven patterns that represent relationships between input parameters and process results, including interactions between the parameters, to predict the process results according to shared and non-shared parameters. This DDMN consists of three modules: an attention module, a fusion module, and a prediction module. The attention module (AM) is operated as a single node perceptron with a nonlinear activation function, ReLU, for each input parameter. The AM utilizes an

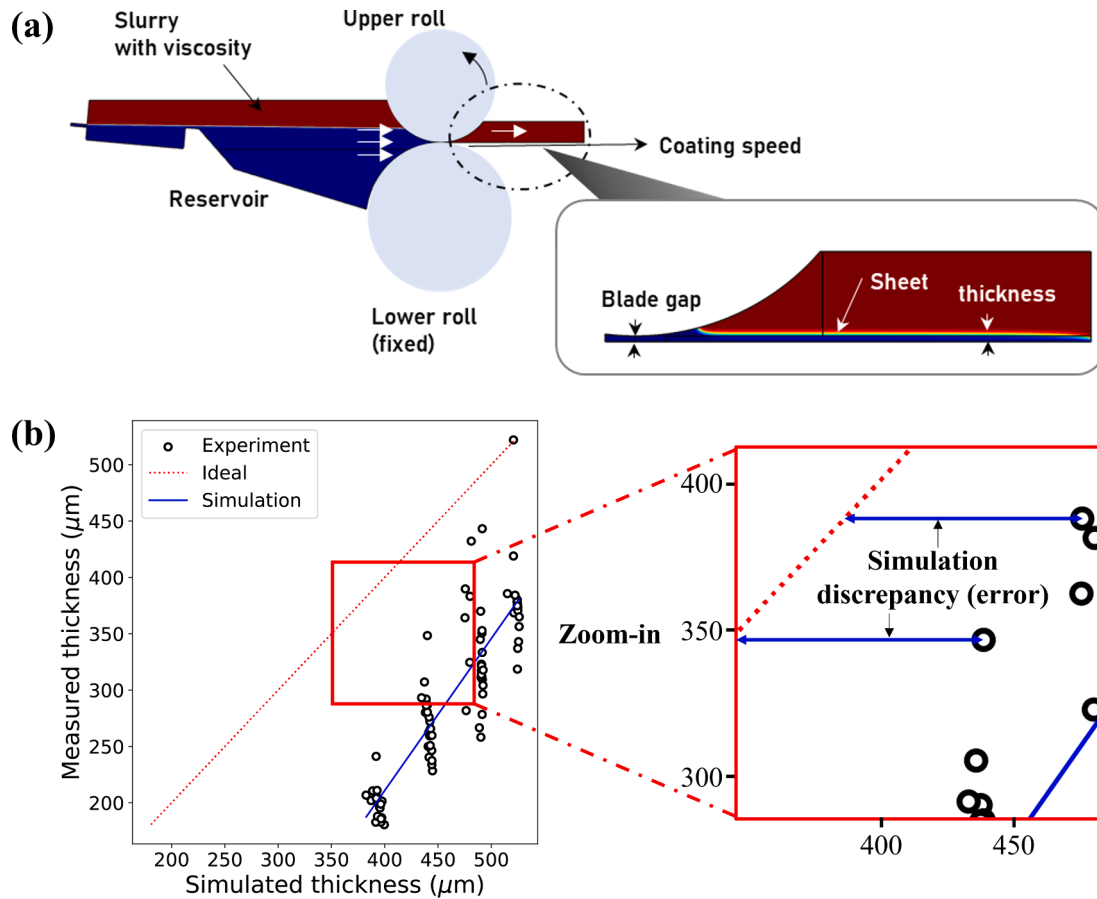


Fig. 2. (a) FEM simulation schematic for the doctor blade part of tape casting process. (b) the residual analysis of the FEM simulation results for the experimental dataset.

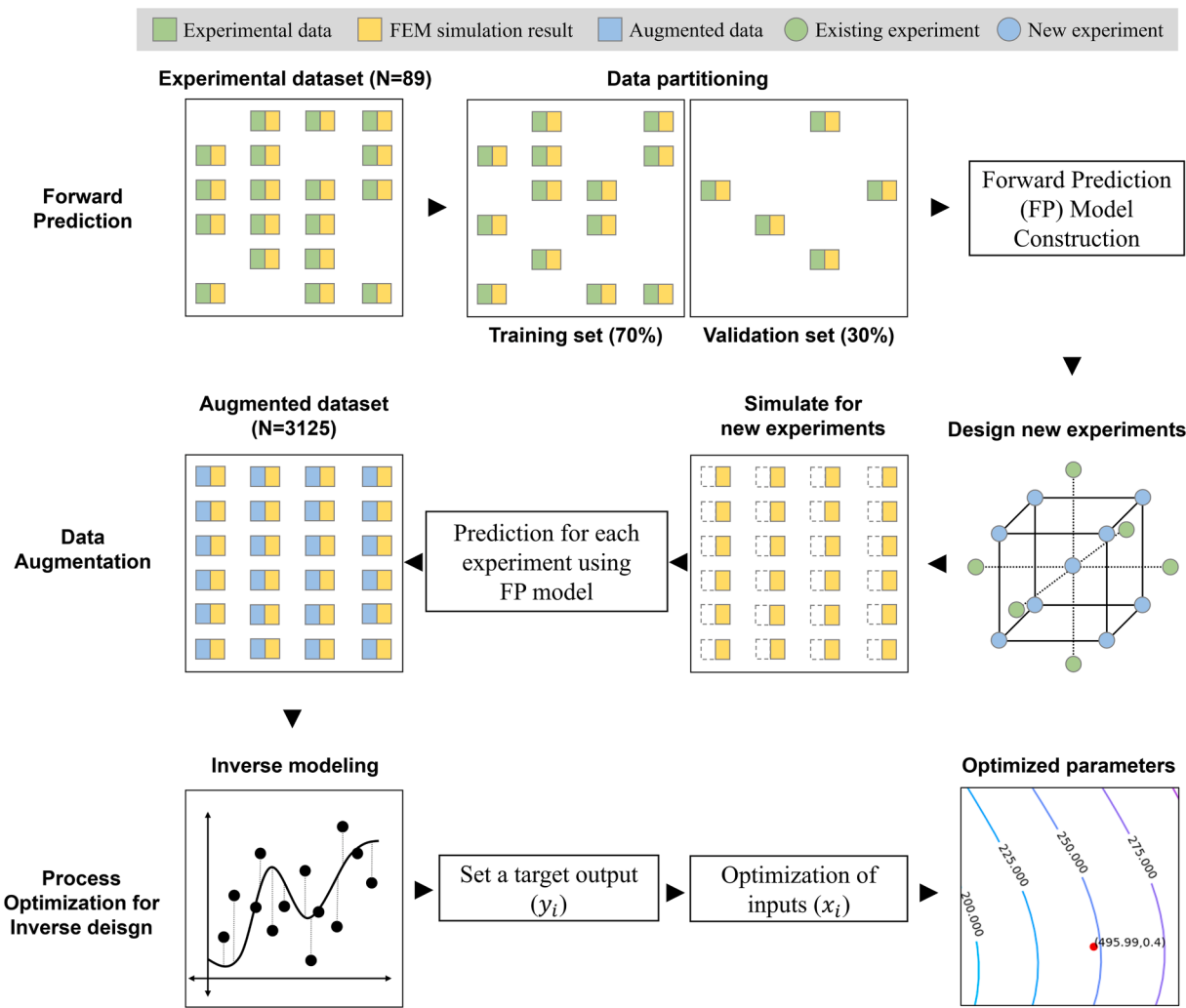


Fig. 3. The overall workflow for the proposed versatile strategy.

attention mechanism that emphasizes the direct effects of each input parameter by learning a relationship between the input parameter and an output. Conversely, the fusion module (FM) is operated as a multi-layer perceptron to extract discriminative representations for the output. With the extracted features from both attention and fusion modules, the prediction module (PM) learns by approximating a function that predicts the output according to the universal approximation theorem. In particular, the DDMN simultaneously considers the patterns representing the physics of the FEM simulation extracted from the PIN. In other words, the proposed FP model can incorporate the advantages of PBM and DDM through multi-task learning for PIN, which learns physics from FEM simulation, and DDMN, which predicts process results.

Let X be a set of experimental data $\{x_1, x_2, \dots, x_n\}$, and the process and FEM simulation results for an experimental data x_i be $y_{t,i}$ and $y_{s,i}$, respectively. Here, each experimental data x_i consists of d parameters $\{x_{i1}, x_{i2}, \dots, x_{id}\}$. Specifically, in the tape casting process, the experimental data x_i consists of five input parameters $x_{i1}, x_{i2}, x_{i3}, x_{i4}$, and x_{i5} , corresponding to P/B ratio (PBR), binder (BIN), viscosity (VIS), coating speed (SPD), and bladegap (GAP), respectively. For the experimental data x_i , the proposed FP model first feeds $\tilde{x}_i = \{x_{i1}, x_{i4}, x_{i5}\}$, which is only composed of shared parameters, and x_i to PIN and DDMN, respectively. To reflect the nonlinearity between the parameters and outputs, we transform the \tilde{x}_i and x_i using the second-order polynomial transformation function $\Phi(\bullet)$ before feeding them to the PIN and DDMN. Subsequently, the PIN is optimized by minimizing the difference

between the predicted FEM simulation result $y_{s,i}$ from the four dense layers for $\Phi(\tilde{x}_i)$ and the actual FEM simulation result $\hat{y}_{s,i}$. The loss function \mathcal{L}_P of PIN is defined as $|\hat{y}_{s,i} - y_{s,i}|$. On the other hand, the DDMN is optimized by minimizing the difference between the predicted process result $y_{t,i}$ for $\Phi(x_i)$ and the actual process result $\hat{y}_{t,i}$. Here, a result of the tape casting process is sheet thickness. The loss function \mathcal{L}_D of DDMN is defined as $|\hat{y}_{t,i} - y_{t,i}|$. To optimize the PIN and DDMN simultaneously, we define the integrated loss function for multi-task learning as $\mathcal{L} = \lambda \mathcal{L}_P + (1-\lambda) \mathcal{L}_D$, where λ is the weight for the physics in the FEM simulation.

3.2. Data augmentation

Inverse design is mainly achieved through the process optimization. In general, the process modeling based on controllable parameters is preceded to optimize the target process. However, in materials-related domain, the process modeling is often failed because it is overfitted to small experimental data [22]. To avoid this overfitting problem of the process modeling, we augment experimental data by utilizing the proposed FP model. We first design new experimental points, which are homogeneously scattered, based on the design of experiment (DOE) approach, as shown in Fig. 3. These new experimental points correspond to all combinations of process parameters set at five levels. In tape

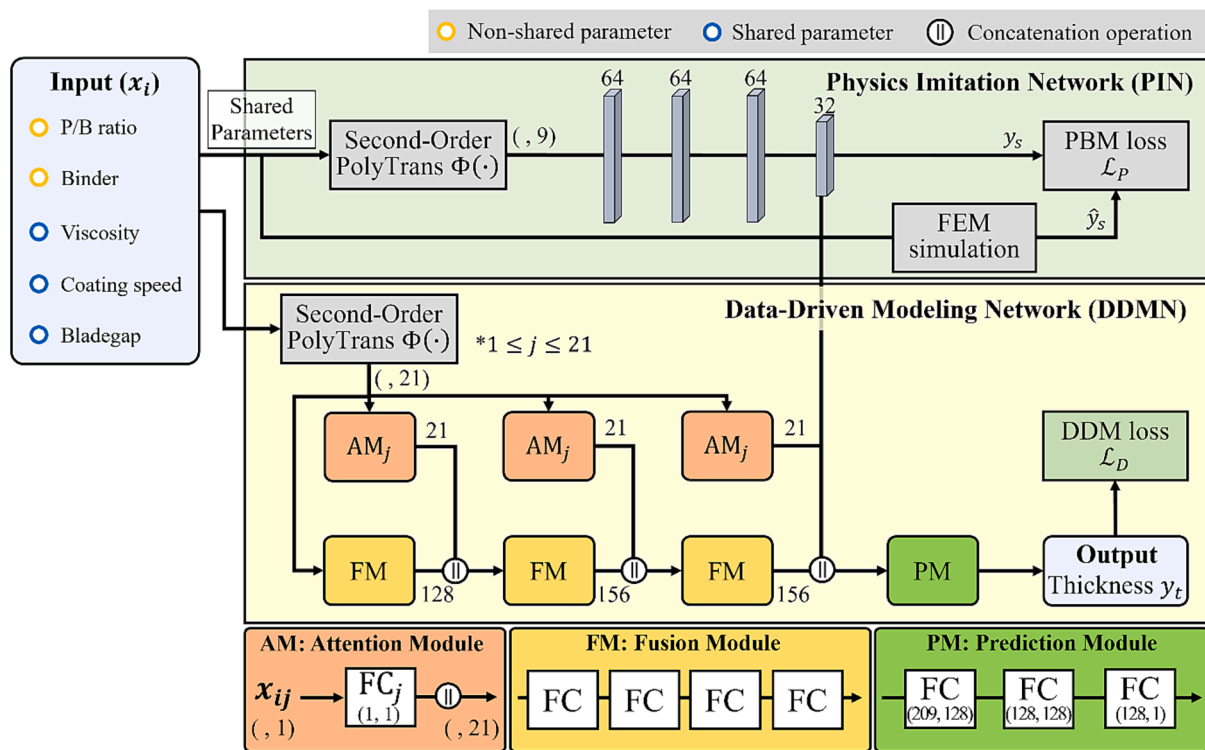


Fig. 4. An architecture of the proposed forward prediction model.

casting process, we determine five levels for each parameter according to the central composite inscribed (CCI) of the DOE. Here, the range of each parameter follows the experimental data. Table 1 shows the levels of the five parameters determined by the DOE.

Afterwards, we calculate the FEM simulation results for the new 3,125 experimental points. Then, we utilize the proposed FP model to predict process results of those experimental points. In particular, the proposed FP model learns data-driven patterns to minimize the discrepancy between the FEM simulation result and the measured process result (thickness) through multi-task learning. In other words, this FP model learns physics that simulate the doctor blade part of the tape casting process from shared parameters, and learns patterns of thickness transformation by drying zone part of the tape casting process from non-shared parameters. Additionally, because the FP model is trained on existing 89 experimental data, it predicts similar process results to those experimental data for the new 3,125 experimental points. Finally, we utilize these 3,125 experimental points with their FEM simulations and predicted process results as augmented experimental data. Fig. 5 shows the discrepancies between the FEM simulation and process results for the augmented experimental data. These augmented experimental data have discrepancies similar to those of the 89 experimental data shown in Fig. 2(b). The result of this residual analysis indicates that the augmented experimental data approximate the physics and patterns of the 89 experimental data.

Table 1
Ranges and levels for five parameters of tape casting process.

Process parameter	Level				
	-2	-1	0	1	2
x_{*1} : P/B ratio (%)	0.3	0.34	0.45	0.56	0.6
x_{*2} : binder (g)	10	15.34	30	44.66	50
x_{*3} : viscosity (cP)	1,000	2,070	5,000	7,930	9,000
x_{*4} : coating speed (m/min)	0.5	0.7	1.25	1.8	2
x_{*5} : bladegap (μm)	300	380	600	820	900

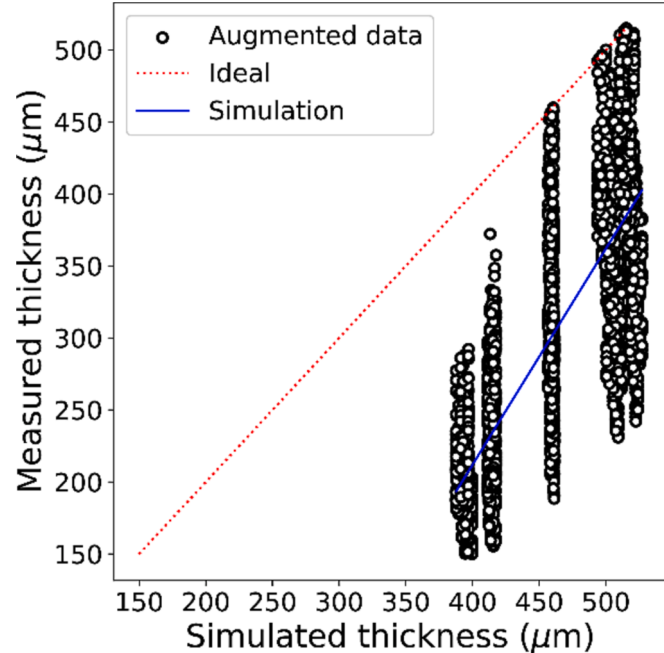


Fig. 5. The residual analysis for the FEM simulation results of augmented experimental data.

3.3. Process optimization for inverse design

With the augmented experimental data, we perform the process optimization to achieve an inverse design. To optimize the process, we first conduct process modeling by utilizing second-order polynomial regression model. This regression model can interpret the linear and non-linear relationships between five process parameters and the process result. Therefore, we formulate the process model of tape casting as

following Eq. (1).

$$g(x) = \beta_0 + \sum_{p=1}^6 \beta_p x_{\bullet p} + \sum_{p=1}^6 \beta_{pp} x_{\bullet p}^2 + \sum_{p < q} \beta_{pq} x_{\bullet p} x_{\bullet q} + \epsilon \quad (1)$$

where β_0 is an intercept, and β_p , β_{pp} , and β_{pq} are regression coefficients corresponding to main, quadratic, and interaction effect terms, respectively. ϵ is an error term which aggregates all possible errors such as the error for process parameters that are not considered, the error caused by the process modeling using second-order polynomial regression model, and the error of data augmentation. Here, we determine terms to remove based on the p -value in the second-order polynomial regression model; the regression coefficients of the terms with large p -values have huge variances, and thus, their precision is degraded. In general, regression terms with p -values of 0.05 or less can reject the null hypothesis and are statistically significant, thereby we use the second-order polynomial regression model consisting of only these significant terms.

After constructing the regression model, we can optimize the five process parameters by the gradient-based optimization method. More precisely, we formulate this optimization problem as the following objective function, $\mathcal{O}(x_i) = |y_{t,i} - g(x_i)|$, where $y_{t,i}$ denotes an actual process result (i.e., thickness) for i -th input data x_i and $g(x_i)$ denotes a predicted process result of the second-order polynomial regression model. We achieve process optimization by finding the solution $\bar{x} = \operatorname{argmin}_x \mathcal{O}(x)$, and various optimization approaches can be applied, this paper adopted the particle swarm optimization (PSO) approach [23] to find the optimal solution. The PSO approach searches for the global optimal solution of the objective function through the swarming behavior of individuals that mimics the social behavior of bird flocks. The behavior of each particle depends on its own experience and the social experience of other particles, and the particles converge from random positions to a specific position corresponding to the global optimal solution. With this optimization, we find the most probabilistically optimal solution in the input domain space.

4. Results and discussion

4.1. Experimental setting

In this section, to evaluate the performance, the proposed strategy is applied to the 89 experimental data gathered from the target tape casting process. We analyze the effectiveness of our proposed strategy for process modeling and optimization, incorporating the advantages of PBM and DDM, through ablation studies on FEM simulation. In addition, to present the superiority of the proposed strategy, we conduct comparative experiments for linear regression (LR), random forest (RF), and deep neural networks (DNN), which are the baselines of linear, ensemble, and deep learning-based DDMs, respectively. These competing methods, including ours, are evaluated by R-squared scores for the results of forward prediction (i.e., thickness prediction), inverse design for shared parameters, and inverse design for non-shared parameters.

To implement the proposed forward prediction (FP) model in our strategy, we utilize the FEM simulation modeled by the COMSOL Multiphysics package. In training step, we use stochastic gradient descent with a momentum score of 0.9 to optimize the proposed FP model. The batch size N is 8. The initial learning rate is set to 0.1 and decreases by 0.1 times when the performance on the validation set saturates. The total training epoch is set to 500. The weight of the physics of FEM simulation λ is set to 0.5. On the other hand, RF and LR were provided from scikit-learn, a Python library, and DNN is implemented as a naïve architecture consisting of four perceptron layers. Here, DNN utilize the same optimizer and objective function as the proposed FP model in our strategy. We repeat 100 iterations for all experiments with the same

training and test sets.

4.2. Result of process modeling

In this subsection, we evaluate the results of process modeling on augmented experimental data according to the proposed strategy. Fig. 6 shows the results of the residual analysis for the tape casting process modeled by second-order polynomial regression. Fig. 6(a) illustrates a scatter plot between actual thickness y_t and predicted thickness $g(x)$ for 89 experimental data. In Fig. 6(a), black points correspond to coordinates $(y_{t,i}, g(x_i))$, $i = 1, \dots, 89$, and dotted red and thick blue lines represent the straight line $y_t = g(x)$ and least squares fitted line to the black points, respectively. A strong linear correlation between y_t and $g(x)$ indicates that our process model (i.e., second-order polynomial regression model) can interpret the tape casting process adequately. Fig. 6(b) shows a scatter plot for adjacent pairs of residuals (r_{i-1}, r_i) to analyze the independence for residuals of the process model. Here, a residual r_i is $y_{t,i} - g(x_i)$. As shown in Fig. 6(b), our process model satisfies the independence assumption because there is no clear positive or negative correlation between r_{i-1} and r_i . Fig. 6(c) shows a scatter plot between $g(x_i)$ and r_i to analyze the homoscedasticity for the residuals of the process model. The $g(x_i)$ and r_i are independent, indicating that our process model is trained homogeneously in overall prediction ranges. Fig. 6(d) illustrates the line plot of the residuals to analyze their white noise properties. As shown in Fig. 6(d), the sample mean of the residuals is almost zero, and their irregular behavior is observed. Therefore, our process model is well generalized because its residuals have white noise properties. Fig. 6(e) shows that the residuals of the process model do not depart from the symmetry and normality severely. To sum up, from Fig. 6, we can conclude that the second-order polynomial regression model with augmented experimental is homogeneously trained in overall prediction ranges, and the process model can sufficiently interpret the tape casting process with high precision.

On the other hand, we conduct an ablation study for FEM simulation to analyze the parameter significance of our process model. Through this ablation study, we analyze the effectiveness of the FEM simulation to the process modeling. To do this, we utilize four different measures to accurately evaluate the parameter significance of the process model.

- Linear correlation (LC): it represents the linear correlation between each parameter $x_{\bullet j}$ ($1 \leq j \leq 5$) and the predicted thickness $g(x_{\bullet})$, and corresponds to the Pearson correlation coefficient.
- Non-linear correlation (NC): it represents the non-linear correlation between each parameter $x_{\bullet j}$ ($1 \leq j \leq 5$) and the predicted thickness $g(x_{\bullet})$, and corresponds to the distance correlation coefficient.
- GINI coefficient: it indicates how well a target $y_{t,\bullet}$ is distinguished and specified by the parameter $x_{\bullet j}$ ($1 \leq j \leq 5$), similar to the entropy of information theory.
- Shapley additive explanations (SHAP) value: it is one of the visualization tools for interpreting the analytical model, which indicates the contribution of each parameter $x_{\bullet j}$ ($1 \leq j \leq 5$) to predicting a process result.

Fig. 7 shows results of significance analysis for the five process parameters. As shown in Fig. 7(a), the parameter significance of the process model excluding the FEM simulation is consistently biased toward the bladegap (GAP). In particular, LC and NC of other parameters except for viscosity (VIS) and GAP are less than 0.1, and thus, these parameters are irrelevant to the process result. In particular, the GINI of the four parameters excluding GAP is less than 0.1, which means that it is difficult to distinguish different process results with only the four parameters. Therefore, inverse design using the process model excluding the FEM simulation is not suitable for the remaining parameters except for GAP. On the other hand, as shown in Fig. 7(b), the parameter significance of the process model utilizing the FEM simulation is relatively

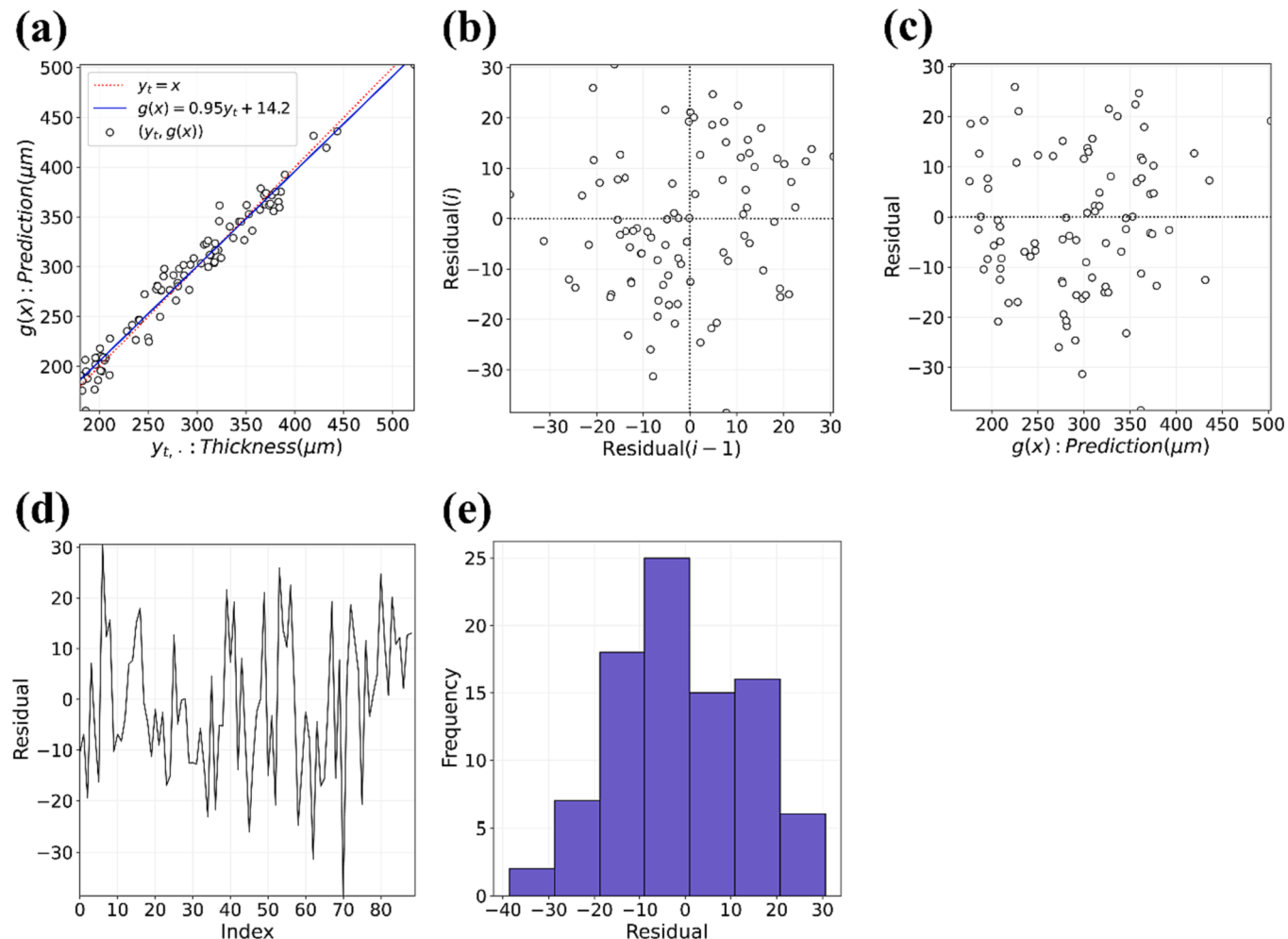


Fig. 6. The results of residual analysis for the process model: (a) scatter plot between actual thickness and predicted thickness; (b) the result of independence analysis; (c) the result of homoscedasticity analysis; (d) the result of the white noise property analysis; (e) the result of normality.

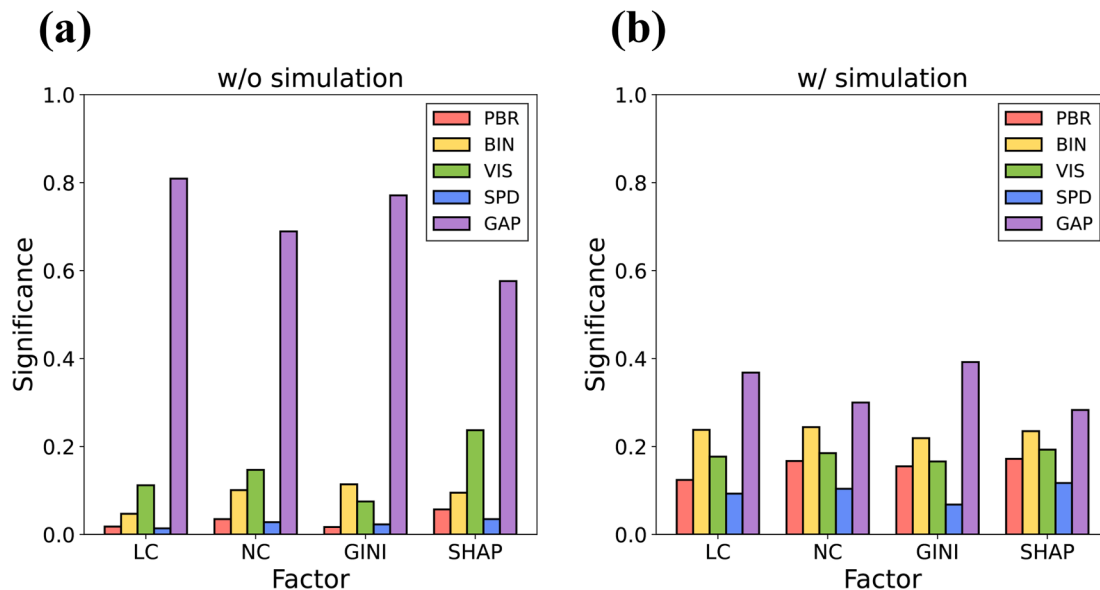


Fig. 7. Parameter significance for the process model: (a) experimental results without the FEM simulation; (b) experimental results with the FEM simulation.

well-distributed. Although GAP remains the most significant, other parameters also have significant correlations and contribute to distinguishing and predicting process results. These experiments imply that FEM simulations make a positive contribution to process modeling; and thus, our proposed strategy combining the advantages of PBM and DDM improves the performance of the inverse design.

Fig. 8 shows the response surface of the modeled tape casting process. The optimal parameters for a target process result can be found by conducting process optimization based on the response surface. **Fig. 8(a)** illustrates the response surface of the process model excluding the FEM simulation. As shown in **Fig. 8(a)**, the response surface shows negative relationships for P/B ratio (PBR) and positive relationships for viscosity (VIS), coating speed (SPD), and bladegap (GAP). It shows a non-linear relationship to binder (BIN). However, these relationships are different from those observed for 89 experimental data (detailed in SI. 1), resulting in the degradation of the performance for the inverse design. Conversely, **Fig. 8(b)** shows the response surface of our process model using the FEM simulation. In the response surface of this process model, the relationships for the process parameters excluding BIN match those for the 89 experimental data. In the response surface of this process model, BIN shows a negative relationship because BIN is utilized to reduce the discrepancy between the result of FEM simulation and actual thickness in the proposed FP model. Despite the different in the relationship to BIN, our process model can increase the parameter significance of BIN, thereby improving the performance of the inverse design.

4.3. Result of parameter optimization

In this subsection, we evaluate the process modeling and optimization performance of the proposed strategy. **Fig. 9** shows the results of the

performance evaluation for the forward prediction and inverse design. In **Fig. 9(a)**, our process model improves the performance of the inverse design by about 16 % when FEM simulation is utilized. In particular, the performance of the inverse design for non-shared parameters is dramatically improved by about 42.6 %. This result indicate that the physics of FEM simulation contributes positively to DDM and our strategy for inverse design is valid. Furthermore, it is worth noting that the discrepancy between the results of the FEM simulation and the actual thickness is effective in process modeling for non-shared parameters that are not considered in the FEM simulation. **Fig. 9(b)** illustrates the results of comparative experiments for four competing methods. In **Fig. 9(b)**, our process model outperforms other competing methods for the forward (thickness) prediction and inverse design. Interestingly, the DNN utilized deep learning similar to the proposed FP model in our strategy, but achieved the worst performance of the forward prediction and inverse design. These results indicate that the network architecture for multi-task learning of the proposed FP model is more effective for process modeling than DNN.

Fig. 10 shows the results of the process optimization for the tape casting process modeled by the proposed strategy. The target thickness for process optimization was set to 300 μm . **Fig. 10(a)** shows the trajectories of each parameter in the optimal solution. In the initiation step to find the optimal solution, there are some fluctuations. Afterwards, the search process is repeated according to the PSO approach, and then each parameter is converged to a specific value. Interestingly, the optimal solution depends on whether or not FEM simulation is utilized because the response surfaces is deformed by the FEM simulation. **Fig. 10(b)** and 10(c) illustrate the optimal solutions of the process model excluding FEM simulation and the process model utilizing FEM simulation, respectively. Unlike the process model excluding FEM simulation, our

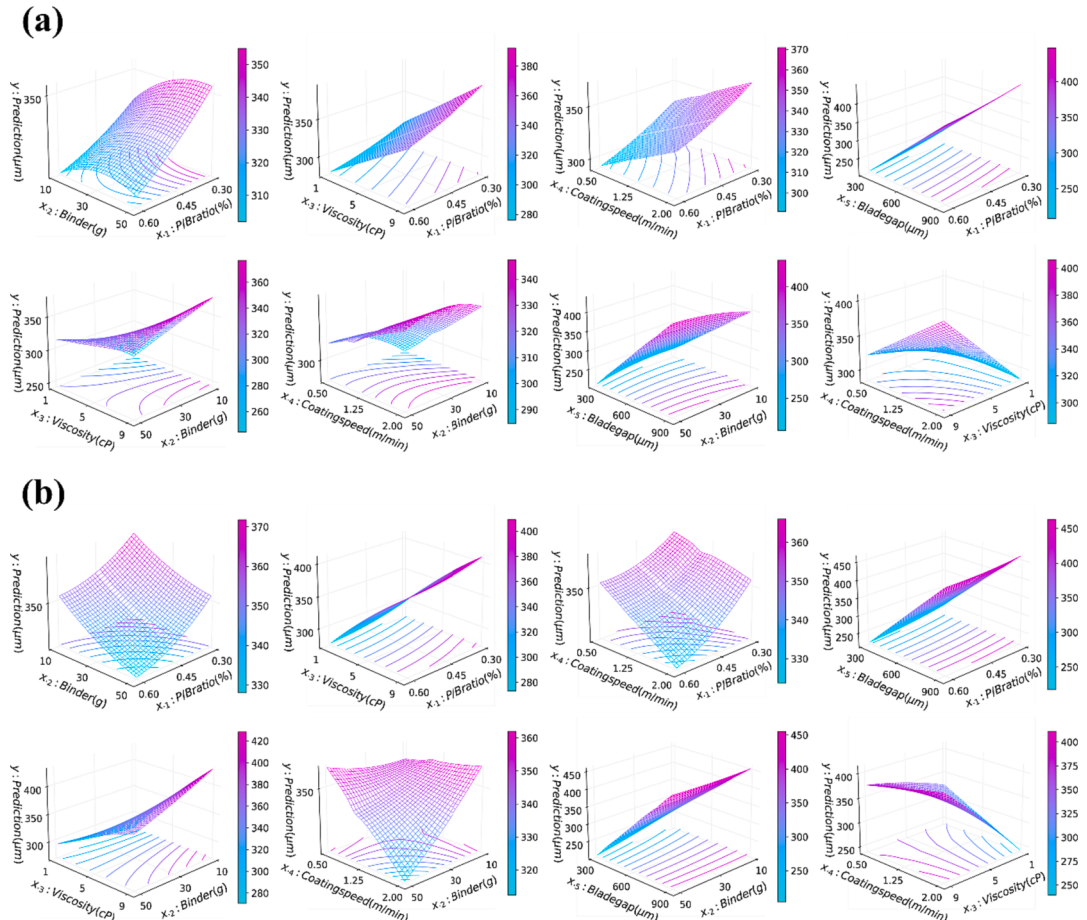


Fig. 8. Response surface plots for the process model: (a) the process model without FEM simulation; (b) the process model with FEM simulation.

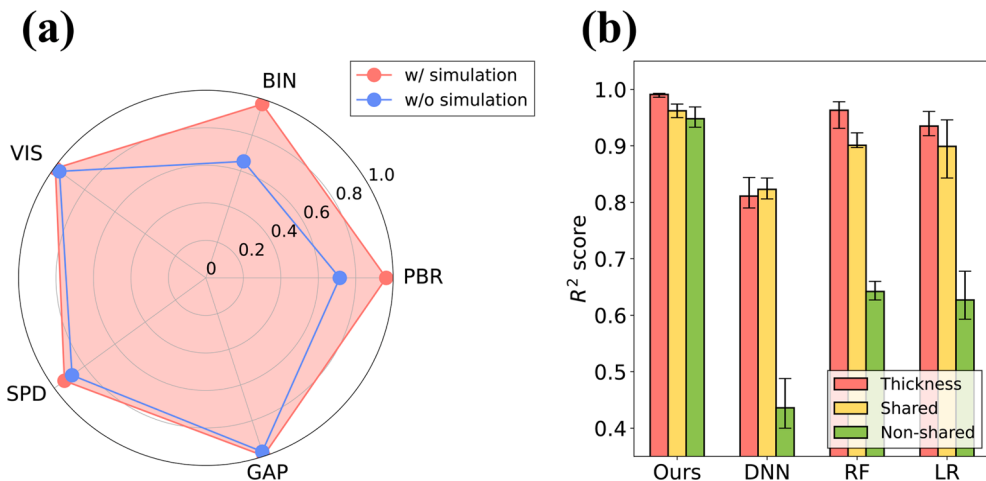


Fig. 9. The results of comparative experiments: (a) the performance of the proposed strategy for the inverse design; (b) the performance of the forward prediction and inverse design for each competing method.

process model utilizing FEM simulation is close to the target thickness (300 μm). On the other hand, the process model excluding FEM simulation converges to an optimal solution with an error of about 28 μm from the target thickness. This result indicate that our proposed strategy performs an accurate inverse design for the target thickness. Fig. 10(d) and 10(e) show photographs of sheets produced according to the optimal solutions of the two process models, respectively. The white regions on the sheet are cracks and indicate a defective product.

4.4. Effectiveness for small dataset

In this subsection, we analyze the effectiveness of the proposed strategy on small experimental data. In Fig. 11, the R-squared scores of our method with different number of training data n are demonstrated. To select n training data from 89 experimental data, we find the centroids of n clusters using k -means clustering. These centroids can be regarded as representatives. Consequently, and surprisingly, we observed that the R-squared scores of the forward prediction were robust to the number of training data when our process model utilized the FEM simulation. On the other hand, as shown in Fig. 11(a), the process model excluding the FEM simulation achieved poor R-squared scores for the inverse design of shared and non-shared parameters regardless of the number of training data. Conversely, the process model utilizing the FEM simulation achieved R-squared scores above 0.85 regardless of the number of training data, as shown in Fig. 11(b). In particular, it is worth noting that the process model utilizing FEM simulation, even when trained with only 40 training data, provides a better inverse design than the process model excluding FEM simulation learned with more training data. These results indicate that the process model combining PBM and DDM is more effective in inverse design for shared parameters as well as non-shared parameters than DDM-based process model. In addition, the process model that combines PBM and DDM can provide a stable inverse design even for a relatively small number of training data.

4.5. Discussion

The key concept of presented strategy is to leverage to augment data in homogeneous manner. In previous studies, there have been several optimization approaches by feeding the process parameters stochastically to the ‘forward prediction’ ML models [24,25]. However, these models had limitations: (1) the accuracy is significantly lowered when the training data is insufficient [26,27], and (2) it is time-consuming to search the parametric space and frequently ceases on the local optimization point (e.g., active DOE [28], sequential approximate optimization

[29], or Bayesian optimization [30]), which required additional strategies to address this issue. For the suggested model, it is possible to immediately recommend process parameters with small number of obtained data from real-world, with the presence of a simulation model albeit the model can be simple. The FEM simulation utilized in this study is only partial model of the entire tape casting process, but proven to effectively improve the process modeling; this leads to another key point of this strategy that the simulation model can be partial and concise, as long as it contains essential physics. It has been shown that augmented experimental data generated by the proposed FP model that analyzes partial but core physical phenomena can enforce constraints between input and output variables to incorporate multi-physics knowledge. As a result, it has been shown that the augmented experimental data is capable of generating accurate inverse design (i.e., being sufficiently helpful in recommending process parameters) in complex systems, with our versatile strategy.

The major impact of our study on the versatile strategy are improving predictability of both property and recipe for tape casting process, and methodologically introduced data augmentation to achieve the improvement. The tape casting process is a long-studied process, and there has been various studies on physics-based interpretation [31,32]. However, these studies may not be able to account for all the factors beyond the physical model. The results from our versatile strategy enabled a successful theoretical prediction beyond the modeled PBM system. Furthermore, although there have been basic feature engineering techniques applied using descriptors [33,34], this particular study stands out for introducing a methodology involving data augmentation. This novel approach has significant ramifications for the domain of material processing and manufacturing, as it presents a systematic way of resolving chronological issue of data deficiency in experiments and industries. To sum up, this work envisages our versatile strategy being applicable to numerous experiments and industrial applications.

5. Conclusion

In this work, we have demonstrated that the inverse design even with a small amount of experimental data (less than a hundred) is viable with the proposed strategy. The homogeneously augmented dataset with both real-lift-measurement model and physics-inspired computational model allowed the successful process parameter optimization. Astonishingly, the optimization performance was even decent for non-shared parameters that were not considered in computational model; R-squared values of 0.97 and 0.96 for shared and non-shared parameters, respectively. Furthermore, our study showed that even if there is a model including only few core physics, and even if a model ascribes partial

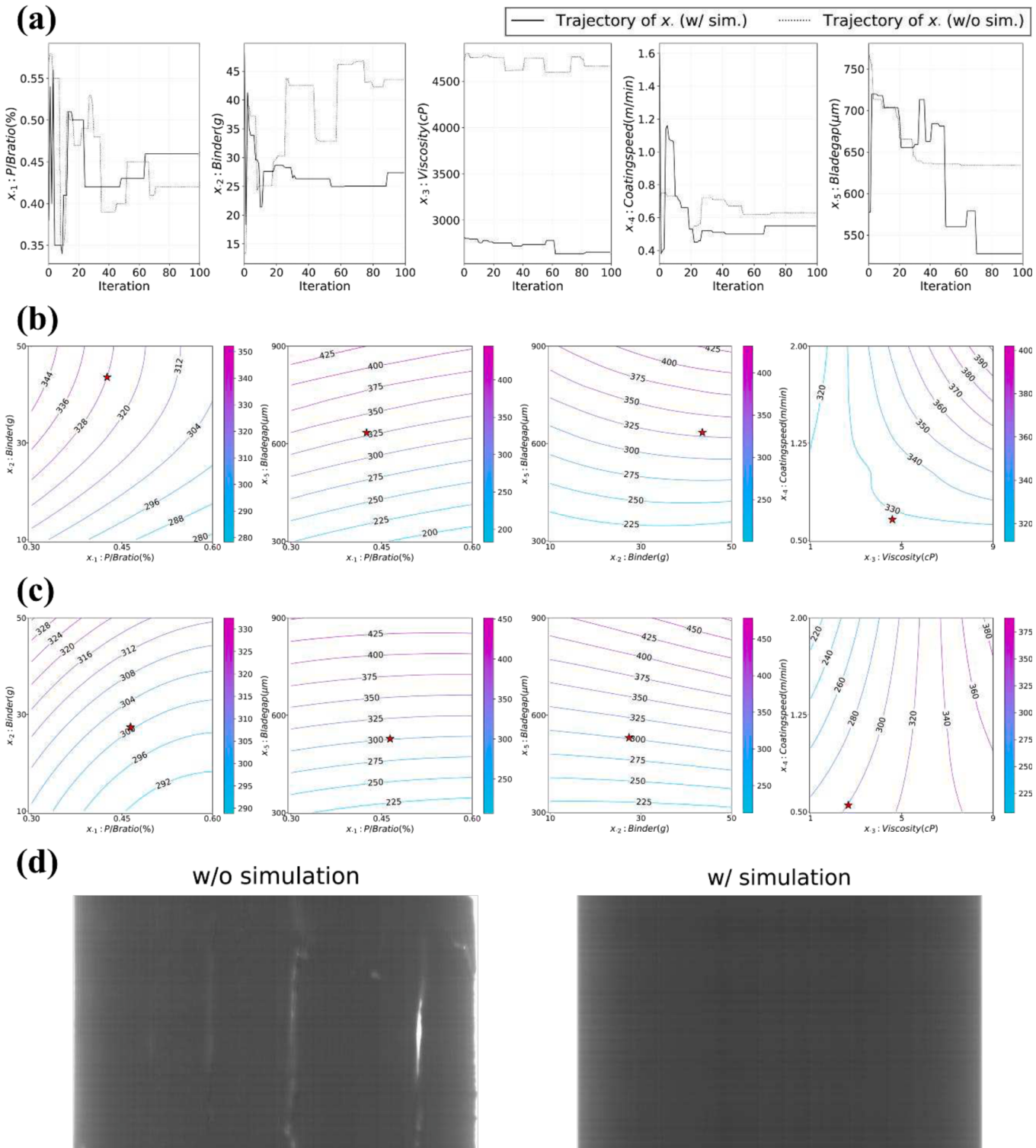


Fig. 10. The results of process optimization for process models: (a) the trajectories of five process parameters in the optimal solution; (b) the contour plot for the process model excluding FEM simulation; (c) the contour plot for the process model utilizing FEM simulation; (d) photographs of the sheets produced according to the optimal solutions.

process, it is possible to establish a reliable process parameter optimization.

By combining the strengths of physics-based modeling (PBM) and data-driven modeling (DDM), we were able to generate accurate inverse models that can recommend process parameters in complex manufacturing systems. While attempts to implement of theoretical or

physical information combined with machine learning for material development [11–13], this is one of the early cases where machine learning was applied to incorporate physical information into processes. Furthermore, although there have been basic feature engineering techniques applied using descriptors [33,34], this particular study stands out for introducing a methodology involving data augmentation. This novel

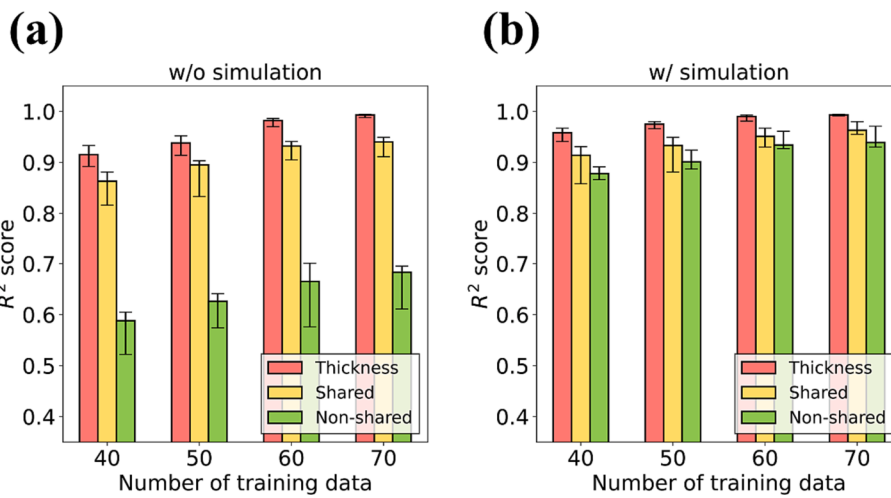


Fig. 11. Performance evaluation of the forward prediction and inverse design of proposed strategy according to the number of training data.

approach has significant ramifications for the domain of material processing and manufacturing, as it presents a systematic way of enhancing manufacturing processes that can be adapted to a wide range of experiments and industrial settings. To sum up, this work envisages our versatile strategy being applicable to numerous experiments and industrial applications.

CRediT authorship contribution statement

Jeong-Hun Kim: Methodology, Investigation, Writing – original draft. **Hyunseok Ko:** Methodology, Investigation, Writing – original draft. **Dong-Hun Yeo:** Resources, Data curation. **Zeehoon Park:** Resources. **Upendra Kumar:** Data curation. **Kwan-Hee Yoo:** Supervision. **Aziz Nasridinov:** Conceptualization, Writing – review & editing, Project administration. **Sung Beom Cho:** Conceptualization, Writing – review & editing, Project administration, Funding acquisition.

Declaration of Competing Interest

The authors declare that they have no known competing financial interests or personal relationships that could have appeared to influence the work reported in this paper.

Data availability

Data supporting the findings of this study are available on request from the corresponding authors. The data are not publicly available due to them containing information that could compromise research participant privacy/consent.

Acknowledgement

We acknowledge the support from Ministry of Trade, Industry & Energy (20004367) and National Research Foundation (RS-2023-00209910). This research was also supported by the MSIT(Ministry of Science and ICT), Korea, under the Grand Information Technology Research Center support program(IITP-2023-2020-0-01462) supervised by the IITP(Institute for Information & communications Technology Planning & Evaluation). The computations were carried out using resources from Korea Supercomputing Center (KSC-2022-CRE-0348).

Appendix A. Supplementary data

Supplementary data to this article can be found online at <https://doi.org/10.1016/j.matdes.2023.112357>.

References

- [1] S. So, T. Badloe, J. Noh, J. Bravo-Abad, J. Rho, Deep learning enabled inverse design in nanophotonics, *Nanophotonics*. 9 (2020) 1041–1057.
- [2] A. Zunger, Inverse design in search of materials with target functionalities, *Nat. Rev. Chem.* 2 (2018) 0121.
- [3] M. Zhou, A. Vassallo, J. Wu, Toward the inverse design of MOF membranes for efficient D2/H2 separation by combination of physics-based and data-driven modeling, *J. Membr. Sci.* 598 (2020), 117675.
- [4] G.E. Karniadakis, I.G. Kevrekidis, L. Lu, P. Perdikaris, S. Wang, L. Yang, Physics-informed machine learning, *Nature Rev. Phys.* 3 (2021) 422–440.
- [5] E. Bedolla, L.C. Padilla, R. Castaneda-Priego, Machine learning for condensed matter physics, *J. Phys. Condens. Matter* 33 (5) (2021), 053001.
- [6] Y.-Y. Zhang, W. Gao, S. Chen, H. Xiang, X.-G. Gong, Inverse design of materials by multi-objective differential evolution, *Comput. Mater. Sci.* 98 (2015) 51–55.
- [7] D. Morgan, R. Jacobs, Opportunities and Challenges for Machine Learning in Materials Science, *Annu. Rev. Mat. Res.* 50 (1) (2020) 71–103.
- [8] J. Cai, X. Chu, K. Xu, H. Li, J. Wei, Machine learning-driven new material discovery, *Nanoscale Adv.* 2 (8) (2020) 3115–3130.
- [9] L. Himanen, A. Geurts, A.S. Foster, P. Rinke, Data-Driven Materials Science: Status, Challenges, and Perspectives, *Adv. Sci.* 6 (2019) 1900808.
- [10] F.J. Montáns, F. Chinesta, R. Gómez-Bombarelli, J.N. Kutz, Data-driven modeling and learning in science and engineering, *Comptes Rendus Mécanique*. 347 (11) (2019) 845–855.
- [11] C. Shen, C. Wang, X. Wei, Y. Li, S. van der Zwaag, W. Xu, Physical metallurgy-guided machine learning and artificial intelligent design of ultrahigh-strength stainless steel, *Acta Mater.* 179 (2019) 201–214.
- [12] P. Singh, T. Del Rose, G. Vazquez, R. Arroyave, Y. Mudryk, Machine-learning enabled thermodynamic model for the design of new rare-earth compounds, *Acta Mater.* 229 (2022), 117759.
- [13] J. Peng, Y. Yamamoto, J.A. Hawk, E. Lara-Curzio, D. Shin, Coupling physics in machine learning to predict properties of high-temperatures alloys, *npj Comput. Mater.* 6 (2020) 141.
- [14] N.V. Chawla, K.W. Bowyer, L.O. Hall, W.P. Kegelmeyer, SMOTE: Synthetic Minority Over-sampling Technique, *J. Artif. Intell. Res.* 16 (2002) 321–357.
- [15] I. Goodfellow, J. Pouget-Abadie, M. Mirza, B. Xu, D. Warde-Farley, S. Ozair, et al., Generative adversarial nets, *Adv. Neural Inf. Procs. Syst.* 27 (2014).
- [16] M.O. Shabani, A. Mazahery, Application of Finite Element Model and Artificial Neural Network in Characterization of Al Matrix Nanocomposites Using Various Training Algorithms, *Metall. Mater. Trans. A* 43 (6) (2012) 2158–2165.
- [17] L. Liang, M. Liu, C. Martin, W. Sun, A deep learning approach to estimate stress distribution: a fast and accurate surrogate of finite-element analysis, *J. R. Soc. Interface* 15 (138) (2018) 20170844.
- [18] D.-C. Chen, C.-S. You, M.-S. Su, Development of professional competencies for artificial intelligence in finite element analysis, *Interact. Learn. Environ.* 1–8 (2020).
- [19] P. Vurtur Badarinath, M. Chierichetti, K.F. Davoudi, A Machine Learning Approach as a Surrogate for a Finite Element Analysis: Status of Research and Application to One Dimensional Systems, *Sensors* 21 (2021) 1654.
- [20] G. Garberoglio, A.I. Skoulias, J.K. Johnson, Adsorption of Gases in Metal Organic Materials: Comparison of Simulations and Experiments, *J. Phys. Chem. B* 109 (2005) 13094–13103.
- [21] H. Kim Dong, Y. Kim Shi, S. Lee Joo, D.-H. Yeo, H.-S. Shin, S.-O. Yoon, Optimization of Alumina Tape Casting Process for Building Big Data, *Journal of the Korean Institute of Electrical and Electronic Material Engineers*. 32 (2019) 483–489.
- [22] Yarlagadda PKDV, Cheng Wei Chiang E. A neural network system for the prediction of process parameters in pressure die casting. *Journal of Materials Processing Technology*. 1999;89-90:583-90.

- [23] M.R. Bonyadi, Z. Michalewicz, Particle Swarm Optimization for Single Objective Continuous Space Problems: A Review, *Evolutionary Computation*. 25 (1) (2017) 1–54.
- [24] D. Xue, P.V. Balachandran, J. Hogden, J. Theiler, D. Xue, T. Lookman, Accelerated search for materials with targeted properties by adaptive design, *Nat. Commun.* 7 (2016) 11241.
- [25] S. Liu, A.P. Stebner, B.B. Kappes, X. Zhang, Machine learning for knowledge transfer across multiple metals additive manufacturing printers, *Addit. Manuf.* 39 (2021), 101877.
- [26] M. Abdul Lateh, A. Kamilah Muda, Z. Izzah Mohd Yusof, N. Azilah Muda, M. Sanusi Azmi, Handling a Small Dataset Problem in Prediction Model by employ Artificial Data Generation Approach: A Review, *J. Phys. Conf. Ser.* 892 (2017), 012016.
- [27] G.-J. Qi, J. Luo, Small Data Challenges in Big Data Era: A Survey of Recent Progress on Unsupervised and Semi-Supervised Methods, *IEEE Trans. Pattern Anal. Mach. Intell.* 44 (4) (2022) 2168–2187.
- [28] H. Shi, S. Xie, X. Wang, A warpage optimization method for injection molding using artificial neural network with parametric sampling evaluation strategy, *Int. J. Adv. Manuf. Technol.* 65 (1-4) (2013) 343–353.
- [29] S. Kitayama, S. Natsume, Multi-objective optimization of volume shrinkage and clamping force for plastic injection molding via sequential approximate optimization, *Simul. Pract. Theory* 48 (2014) 35–44.
- [30] H. Cheng, H. Chen, Online parameter optimization in robotic force controlled assembly processes. 2014 IEEE International Conference on Robotics and Automation (ICRA), IEEE, 2014.
- [31] Y.T. Chou, Y.T. Ko, M.F. Yan, Fluid flow model for ceramic tape casting, *J. Am. Ceram. Soc.* 70 (10) (1987) C-280–C-282.
- [32] R. Pitchumani, V.M. Karbhari, Generalized fluid flow model for ceramic tape casting, *J. Am. Ceram. Soc.* 78 (9) (1995) 2497–2503.
- [33] D. Dai, T. Xu, X. Wei, G. Ding, Y. Xu, J. Zhang, H. Zhang, Using machine learning and feature engineering to characterize limited material datasets of high-entropy alloys, *Comput. Mater. Sci.* 175 (2020) 109618.
- [34] E. Popova, T.M. Rodgers, X. Gong, A. Cecen, J.D. Madison, S.R. Kalidindi, Process-structure linkages using a data science approach: application to simulated additive manufacturing data, *Integrating Mater. Manuf. Innov.* 6 (1) (2017) 54–68.